Mathematical Biosciences and Engineering

http://www.aimspress.com/journal/MBE

MBE, 16(6): 7688–7706.
DOI: 10.3934/mbe.2019385
Received: 08 May 2019
Accepted: 13 August 2019
Published: 21 August 2019

Research article

Dynamic analysis of wild and sterile mosquito release model with Poincaré map

Yufei Wang[1], **Huidong Cheng**[1,*] **and Qingjian Li**[2]

[1] College of Mathematics and System Sciences, Shandong University of Science and Technology, Qingdao 266590, Shandong, China

[2] College of Foreign Languages, Shandong University of Science and Technology, Qingdao 266590, Shandong, China

* **Correspondence:** Email: chd900517@sdust.edu.cn; Tel: +053288032097.

Abstract: In recent years, the application of impulsive semi-dynamic system in state-dependent feedback control has attracted extensive attention, but most models only discuss their special cases without delving into their complex dynamics. Therefore, we establish the wild and sterile mosquito system with integrated mosquito control, and use the Poincaré map method to conduct a comprehensive analysis of the model dynamics. First, the main properties of Poincaré map such as monotonicity, continuous differentiability, extremum and fixed point are discussed. Second, we prove the existence and stability of boundary periodic solution and study the influence of its parameters on the system. Then the existence and global stability of the order-1 periodic solution and the existence condition of the order-k ($k > 1$) periodic solution are analyzed. Finally, our conclusion is verified by numerical analysis. The results show that the population density of wild mosquitoes can be controlled below the threshold by integrated mosquito control.

Keywords: impulsive semi-dynamic system; integrated mosquito control; Poincaré map; periodic solution

1. Introduction

Pulsed semi-dynamic systems are widely used in the study of biological systems with thresholds, such as biological resource management [1–5] and control of epidemics [6–11], etc. These systems include interactions of continuous and discrete dynamics, where the portion that exhibits discontinuity is called a pulse set, thus producing pulse dynamics. In recent years, the qualitative theory of pulsed semi-dynamic systems has been extensively developed [1, 12–15], using a variety of analytical methods, such as successor functions, Bendixson theorem, etc [16–19]. However, due to the complexity of

state-dependent feedback control, the global dynamics of the state-dependent feedback control model is far from being solved. In order to better study the qualitative theory and dynamic complexity of the state-dependent feedback control model, we use the Poincaré map method to analyze and discuss the model.

The most classic and commonly used method for pest control is chemical control, which involves spraying insecticides to control pests. Due to the widespread use of this method, many pests have developed resistance to insecticides [20–23]. Especially in the summer, when mosquito population get rampant, repeated use of insecticides reduces their effectiveness and control. It takes a long time to use only biological control methods, and factors such as temperature and weather may affect biological control [24–27]. When the number of mosquitoes suddenly increases, it is impossible to control the mosquito population in a timely and effective manner. Therefore, in order to solve these problems, we adopted integrated mosquito control [28–31], that is, the use of both chemical control methods and biological control methods for wild mosquitoes.

The biological control method used in this paper is the sterile insect technique (SIT). In this way, mosquitoes are disturbed by the natural reproduction process, so that the wild mosquitoes is reduced [32–35]. Insect sterility technology uses some physical methods to make male mosquitoes sterile and unable to produce offspring. And these sterile mosquitoes are released into the environment to mate with wild females but not to reproduce. This repeated release of sterile mosquitoes or the release of large numbers of sterile mosquitoes may control wild mosquito population [32, 36–38].

In terms of release methods, many articles used proportional release or continuous release [39–42], and these two release methods have some advantages only when the wild mosquitoes population is small. In the actual environment, the mosquito population may be very large. In order to control wild mosquito population more effectively, we adopt a new release method in which the release of sterile mosquitoes is in proportional to the number of wild mosquitoes when the number of wild mosquitoes is small, and while the release of sterile mosquitoes saturates and approaches a constant when the number of wild mosquitoes increases.

The structure of this paper is as follows: In Section 2, we briefly introduce the model and make qualitative analysis. In Section 3, the definition domain and main properties of Poincaré map are introduced and proved. In Section 4, the existence and stability of periodic solutions are analyzed and proved. In Section 5, we simulate the model to verify our conclusion. Finally, the article is analyzed and summarized.

2. Model formulation

2.1. Wild and sterile mosquitoes release model

In article [43], the release model of wild and sterile mosquitoes using only biological control is proposed as follows:

$$\left\{\begin{array}{l} \left.\begin{array}{l} \dfrac{dw(t)}{dt} = w(t)\left[\dfrac{rw(t)}{w(t)+g(t)} - \varphi_1 - a_1(w(t)+g(t))\right], \\ \dfrac{dg(t)}{dt} = -g(t)\left[\varphi_2 + a_2(w(t)+g(t))\right], \end{array}\right\} w < ET, \\ \left.\begin{array}{l} w(t^+) = w(t), \\ g(t^+) = g(t) + b, \end{array}\right\} w = ET, \end{array}\right. \tag{2.1}$$

where $w(t)$ and $g(t)$ indicate the population densities of wild and sterile mosquitoes at time t respectively. r represents the wild mosquito population birth rate and b represents the sterile mosquitoes release rate. Wild and sterile mosquito populations follow logistic growth without interaction then a_i and φ_i, i=1,2, denote the density-dependent and density-independent death rates respectively.

The model (2.1) using only biological control, is more susceptible to external influences, and cannot control sudden growth or a large number of wild mosquito population in a timely and effective manner. Therefore, we propose the following wild and sterile mosquitoes release model using integrated mosquito control:

$$\left\{\begin{array}{l} \left.\begin{array}{l} \dfrac{dw(t)}{dt} = w(t)\left[\dfrac{rw(t)}{w(t)+g(t)} - \varphi_1 - a_1(w(t)+g(t))\right], \\ \dfrac{dg(t)}{dt} = -g(t)\left[\varphi_2 + a_2(w(t)+g(t))\right], \end{array}\right\} w < ET, \\ \left.\begin{array}{l} w(t^+) = Z_1(D)w(t), \\ g(t^+) = Z_2(D)g(t) + \dfrac{bw}{1+w}, \end{array}\right\} w = ET, \end{array}\right. \tag{2.2}$$

where $Z_1(D), Z_2(D)$ represent the survival part of wild and sterile mosquitoes when D dose of insecticide is administered respectively, and $0 \le Z_1(D) \le 1, 0 \le Z_2(D) \le 1$. While killing wild mosquitoes with insecticides, we inevitably kill a certain number of sterile mosquitoes. Therefore we use the response curves of the two populations for insecticides to be expressed in $Z_1(D) = e^{-k_1 D}$ and $Z_2(D) = e^{-k_2 D}$ respectively [44], where $0 \le k_i \le 1$ represents the pharmacokinetics of insecticides. We release sterile mosquitoes in a ratio-dependent manner, when the density of wild mosquitoes reaches the threshold, sterile mosquitoes are released at a rate of $\frac{bw}{1+w}$. Define $w(0^+)$ and $g(0^+)$ as the initial density of wild mosquitoes and sterile mosquitoes, and assumed the initial density of wild mosquitoes is less than the threshold value of ET. We can set $ET < \frac{r-\varphi_1}{a_1}$.

2.2. The qualitative analysis

In the absence of a pulse, system (2.2) becomes the following:

$$\left\{\begin{array}{l} \dfrac{dw(t)}{dt} = w(t)\left[\dfrac{rw(t)}{w(t)+g(t)} - \varphi_1 - a_1\left(w(t)+g(t)\right)\right], \\ \dfrac{dg(t)}{dt} = -g(t)\left[\varphi_2 + a_2(w(t)+g(t))\right]. \end{array}\right. \tag{2.3}$$

By caculation, we can easily get system (2.3) with only one equilibria point $E(w_0, 0)$, where $w_0 = \frac{r-\varphi_1}{a_1}$. Define the isocline of model (2.3) as follows:

$$L_1 = \frac{-(\varphi_1 + 2a_1 w) + \sqrt{\varphi_1^2 + 4ra_1 w}}{2a_1}.$$

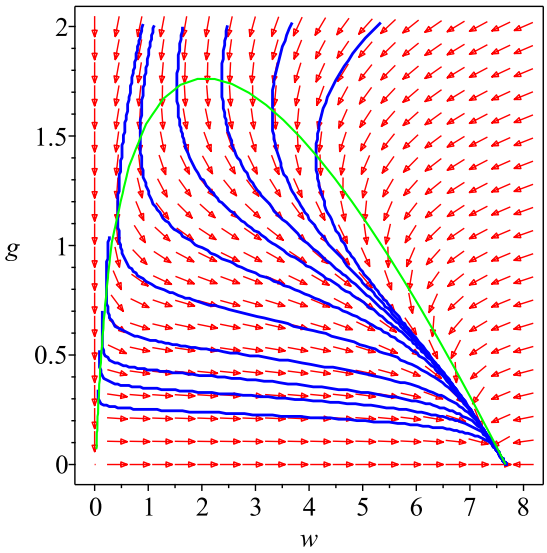

Figure 1. Phase diagram of system (2.3) with $r = 2.5, \varphi_1 = 0.2, a_1 = 0.3, \varphi_2 = 0.01, a_2 = 0.05$.

For model (2.3), the following theorem is satisfied:

Theorem 2.1. *When $r-\varphi_1-2a_1w < 0$, axial equilibrium point $E(w_0, 0)$ is locally asymptotically stable (Fig.1).*

Proof. Let

$$F(w,g) = w\left[\frac{rw}{w+g} - \varphi_1 - a_1(w+g)\right],\ G(w,g) = -g\left[\varphi_2 + a_2(w+g)\right].$$

By calculation, we can obtain

$$\frac{\partial F}{\partial w} = \frac{rwg}{(w+g)^2} + \frac{rw}{w+g} - 2a_1w - a_1g - \varphi_1,\ \ \frac{\partial G}{\partial w} = -a_2g$$

$$\frac{\partial F}{\partial g} = w\left[\frac{-rw}{(w+g)^2} - a_1\right],\ \ \frac{\partial G}{\partial g} = -\varphi_2 - a_2w - 2a_2g.$$

So the jacobian matrix at $E(w_0, 0)$ point is

$$\mathrm{J}(E_1) = \begin{pmatrix} r - \varphi_1 - 2a_1w & -r - wa_1 \\ 0 & -\varphi_2 - a_2w \end{pmatrix}.$$

From the above results, we obtain that when $r - \varphi_1 - 2a_1 w < 0$,

$$\det[\mathrm{J}(E_1)] = (r - \varphi_1 - 2a_1 w)(-\varphi_2 - a_2 w) > 0,$$
$$\mathrm{Tr}[\mathrm{J}(E_1)] = r - \varphi_1 - 2a_1 - \varphi_2 - a_2 w < 0,$$

then $E(w_0, 0)$ is the point of locally asymptotically stable. This completes the proof. □

The following article is discussed under the condition of $r - \varphi_1 - 2a_1 w < 0$ and $b > 0$.

3. The definition and properties of the Poincaré map

First we give the definition of Poincaré map, which is used to study the dynamics of model (2.2). Define the following two lines

$$L_2 : w = e^{-k_1 D} ET,\ L_3 : w = ET.$$

By bringing the $w = ET$ into a straight line L_1, get the intersection of L_1 and L_3, defined as $M_1(ET, g_M)$, where

$$g_M = \frac{-(\varphi_1 + 2a_1 ET) + \sqrt{\varphi_1^2 + 4ra_1 ET}}{2a_1},$$

similarly, the intersection of L_1 and L_2 is defined as $N_1(e^{-k_1 D} ET, g_N)$, where

$$g_N = \frac{-(\varphi_1 + 2a_1 e^{-k_1 D} ET) + \sqrt{\varphi_1^2 + 4ra_1 e^{-k_1 D} ET}}{2a_1}.$$

The set is defined in R_+^2 as follows

$$\Omega = \{(w, g) | 0 < w < ET, g > 0\} \subset R_+^2.$$

Now we define M as the impulse set for model (2.2) $M = \{(w, g) \in \Omega | x = ET, 0 < g < g_M\}$ and M is a closed subset of R_+^2.
While the continuous function is as follows

$$I : (ET, g) \in M \to (w^+, g^+) = (e^{-k_1 D} ET, e^{-k_1 D} g + \frac{bET}{1 + ET}) \in \Omega.$$

Then define the phase set as

$$N = I(M) = \{(w^+, g^+) \in \Omega | w^+ = e^{-k_1 D} ET, \frac{bET}{1 + ET} < g^+ \leq e^{-k_1 D} g_M + \frac{bET}{1 + ET}\}.$$

Without losing generality, we suppose that the initial point (w_0^+, g_0^+) belongs to the phase set. Define the following two sections:

$$W_1 = \{(w, g)|w = ET, g \geq 0\},$$

$$W_2 = \{(w, g)|w = e^{-k_1 D}ET, g \geq 0\}.$$

Choose W_2 as the Poincaré section. Then the trajectory starts at point $S_k^+(e^{-k_1 D}ET, g_k^+) \in L_2$ and intersects with L_3 at the unique point $S_{k+1}(ET, g_{k+1})$. We get g_{k+1} determined by g_k^+ and $g_{k+1} = \sigma(g_k^+)$ from the Cauchy-Lipschitz theorem. Point S_{k+1} goes through one pulse and then it reaches L_2 at point $S_{k+1}^+(e^{-k_1 D}ET, g_{k+1}^+)$ with $g_{k+1}^+ = e^{-k_2 D}g_{k+1} + \frac{bET}{1+ET}$. So we define the Poincaré section as follows

$$g_{k+1}^+ = e^{-k_2 D}\sigma(g_k^+) + \frac{bET}{1 + ET} = P(g_k^+). \tag{3.1}$$

In order to better study the dynamic behavior of system (2.2), we can propose a Poincaré map determined by the pulse point in the phase set according to the definition of the phase diagram. Therefore, we define

$$\begin{aligned} F(w(t), g(t)) &= w(t)\left[\frac{rw(t)}{w(t) + g(t)} - \varphi_1 - a_1(w(t) + g(t))\right], \\ G(w(t), g(t)) &= -g\left[\varphi_2 + a_2(w + g)\right]. \end{aligned}$$

It satisfies a scalar differential equation in a phase space

$$\begin{cases} \dfrac{dg}{dw} = \dfrac{-g\left[\varphi_2 + a_2(w + g)\right]}{w\left[\frac{rw}{w+g} - \varphi_1 - a_1(w + g)\right]} = h(w, g), \\ g(e^{-k_1 D}ET) = g_0^+. \end{cases} \tag{3.2}$$

For model (3.2), we only focus on the regions

$$\Omega_1 = \left\{(w, g)|w > 0, g > 0, g < \frac{-(\varphi_1 + 2a_1 w) + \sqrt{\varphi_1^2 + 4ra_1 w}}{2a_1}\right\}, \tag{3.3}$$

where $h(w, g)$ is continuous and differentiable. And then we define $w_0^+ = e^{-k_1 D}ET, g_0^+ = X, X \in N$. Define

$$g(w) = g(w; e^{-k_1 D}ET, X) = g(w, X), e^{-k_1 D}ET \leq w \leq ET,$$

and from model (3.2), we have

$$g(w, X) = X + \int_{e^{-k_1 D}ET}^{w} h(x, g(x, X)dx. \tag{3.4}$$

Thus, the Poincaré map $P(X)$ can be represented by the following expression

$$P(X) = e^{-k_2 D} g(e^{-k_1 D} ET, X) + \frac{bET}{1 + ET}. \tag{3.5}$$

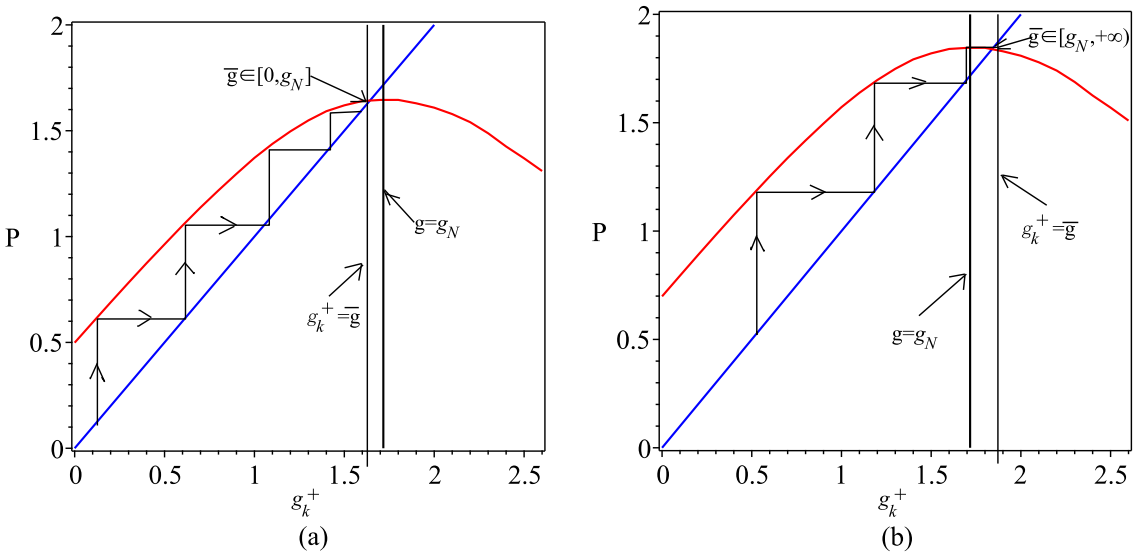

Figure 2. Image of Poincaré map P and the parameters fixed as $r = 2.5, \varphi_1 = 0.2, a_1 = 0.3, \varphi_2 = 0.01, a_2 = 0.05, ET = 2.5.(a)b = 0.7; (b)b = 0.98$.

Next, we prove the main properties of the Poincaré map.

Theorem 3.1. *Poincaré map P has the following properties* (*Fig*.2)
(I) The domain of P is $[0, +\infty)$. *And the Poincaré map P is increasing on* $[0, g_N]$, *decreasing on* $[g_N, +\infty)$.
(II) Poincaré map P is continuously differentiable.
(III)Poincaré map P has a unique fixed point $\overline{g}$.
(IV) When $g_k^+ \to +\infty$, *the Poincaré map P is bounded and there exists horizontal asymptote* $g = \frac{bET}{1+ET}$.
(V)Poincaré map P takes the maximum value at $g = g_N$ *and the maximum value is* $e^{-k_2 D} g(e^{-k_1 D} ET, g_N) + \frac{bET}{1+ET}$; *the minimum value is taken at* $g = 0$, *and the minimum value is* $\frac{bET}{1+ET}$.

Proof. (I) Through qualitative analysis of model (2.3), we get that all trajectories tend to point E_0. After having a pulse, all the trajectories from the phase set eventually reach the pulse set. Therefore, the domain of P is $[0, +\infty)$.

For any point $P_1^+(e^{-k_1 D} ET, g_{p_1}^+)$, $P_2^+(e^{-k_1 D} ET, g_{p_2}^+)$ with $g_{p_1}^+, g_{p_2}^+ \in [0, g_N]$, we assume that $g_{p_1}^+ < g_{p_2}^+$ and $g_{p+1} = \sigma(g_p)$. From the Cauchy-Lipschitz Theorem, $g_{p_1+1} < g_{p_2+1}$ can be obtained. Therefore after one pulse, we get

$$P(g_{p_1}^+) = e^{-k_2 D} g_{p_1+1} + \frac{bET}{1 + ET} < e^{-k_2 D} g_{p_2+1} + \frac{bET}{1 + ET} = P(g_{p_2}^+).$$

Thus P is increasing on $[0, g_N]$.

Similarly, we arbitrarily select two points $Q_1^+(e^{-k_1D}ET, g_{q_1}^+)$, $Q_2^+(e^{-k_1D}ET, g_{q_2}^+)$ with $g_{q_1}^+, g_{q_2}^+ \in [g_N, +\infty)$ and assume that $g_{q_1}^+ < g_{q_2}^+$. The trajectory starts from point Q_1^+, Q_2^+ across the L_2 and then hits the L_3 at points (ET, g_{q_1+1}) and (ET, g_{q_2+1}) , where $g_{q_1+1} > g_{q_2+1}$. After the pulse, we get

$$P(g_{q_1}^+) = e^{-k_2D}g_{q_1+1} + \frac{bET}{1+ET} > e^{-k_2D}g_{q_2+1} + \frac{bET}{1+ET} = P(g_{q_2}^+).$$

Thus P is decreasing on the $[g_N, +\infty)$.

(II) From model (2.3), we get that $F(w, g), G(w, g)$ are continuous and differentiable in the first quadrant. The continuity and differentiability theorems of solutions of ordinary differential equations with respect to their initial conditions are used to determine the differentiability of P. That is, P is continuously differentiable in Ω according to the Cauchy-Lipschitz theorem with parameters.

(III) Since P decreases on $[g_N, +\infty)$, therefore their exists a $g^{'} \in [g_N, +\infty)$ such that $P(g^{'}) < g^{'}$. We can easily obtain $P(0) = \frac{bET}{1+ET} > 0$, then there exists $\overline{g} \in (0, g^{'})$ such that $P(\overline{g}) = \overline{g}$. Therefore P has fixed point on $[0, +\infty)$.

Next we prove the uniqueness of the fixed point. When $P(g_N) < g_N$, the intersection of the phase set and the w axis is defined as $n_0(e^{-k_1D}ET, 0)$, then point n_0 reaches point $(e^{-k_1D}ET, g_{n_0+1}^+)$ after one pulse. And the intersection point $N_1(e^{-k_1D}ET, g_N)$ of L_1 and L_2 reaches the point $(e^{-k_1D}ET, g_{N+1}^+)$ after one pulse. We assume that P has two fixed points $G_1(e^{-k_1D}ET, \overline{g}_1), G_2(e^{-k_1D}ET, \overline{g}_2)$ and $\overline{g}_1, \overline{g}_2 \in (g_{n_0+1}^+, g_{N+1}^+)$ such that $P(\overline{g}_1) = \overline{g}_1, P(\overline{g}_2) = \overline{g}_2$. Since $P(0) = \frac{bET}{1+ET} > 0$, then by the definition of the Poincaré map, we get $P(g) > g$ for $g \in (g_{n_0+1}^+, \overline{g}_1)$. From $P(\overline{g}_1) = \overline{g}_1$, we get for any $g_1^{'} \in (\overline{g}_1, \overline{g}_2)$, $P(g_1^{'}) < g_1^{'}$ holds. And $P(g_2^{'}) < g_2^{'}$ for $g_2^{'} \in (\overline{g}_2, g_{N+1}^+)$ due to $P(g_N) < g_N$ and $P(\overline{g}_2) = \overline{g}_2$. Therefore we obtain $g \in (\overline{g}_1, g_{N+1}^+)$ such that $P(g) < g$, which is a contradiction. So P has a unique fixed point $\overline{g}$ and $\overline{g} \in (0, g_N)$.

Similarly, when $P(g_N) > g_N$, we get that P has unique fixed point $\overline{g}$ and $\overline{g} \in (g_N, +\infty)$.

(IV) Defining the closure of $\overline{\Omega}_1$ as

$$\overline{\Omega}_1 = \left\{ (w, g) | w > 0, g > 0, g \le \frac{-(\varphi_1 + 2a_1w) + \sqrt{\varphi_1^2 + 4ra_1w}}{2a_1} \right\}.$$

$\overline{\Omega}_1$ is the invariant set on system (2.2).

Let

$$L = g - \frac{-(\varphi_1 + 2a_1w) + \sqrt{\varphi_1^2 + 4ra_1w}}{2a_1},$$

if

$$[F(w, g), G(w, g) \cdot (1 - r(\varphi_1^2 + 4ra_1w)^{-\frac{1}{2}}, 1)]_{L=0} \le 0,$$

where $\cdot$ is the product of two scalar vectors, the vector field will enter in $\overline{\Omega}_1$ at the end, that $\overline{\Omega}_1$ is the invariant set. By calculating

$$\dot{V}(x)|_{L=0} = -g(\varphi_2 + a_2(w + g))g + w(\frac{rw}{w + g} - \varphi_1 - a_1(w + g)) = g^2(\varphi_2 + a_2(w + g)) < 0.$$

For all $(w, g) \in \overline{\Omega}_1$, $\frac{dw(t)}{dt} > 0, \frac{dg(t)}{dt} < 0$ holds. So we get $\sigma(+\infty) = 0$ with $(e^{k_1 D}ET, 0) \in N$ and $P(+\infty) = \frac{bET}{1+ET}$. We assume that there exists a positive g_* that makes $\sigma(+\infty) = g_*$ and $P_* = (ET, g_*) \in M$. Take another point $P_1 = (ET, g_1)$ and $0 < g_1 < g_*$. By the invariance of set $\overline{\Omega}_1$ and uniqueness of solution, we get that the orbit initiating P_1 will arrive at point $P_0^+ = (e^{-k_1 D}ET, g_0^+) \in N$ and $g_0^+ > +\infty$, which is a contradiction. Therefore, we obtain $\sigma(+\infty) = 0$ and $P(+\infty) = \frac{bET}{1+ET}$, so P has a horizontal asymptote $P = \frac{bET}{1+ET}$.

(V) From the proof (I), we get that P is increasing on $[0, g_N]$ and decreasing on $[g_N, +\infty)$. And for $\forall \overline{n} \in (0, +\infty)$, $P(\overline{n}) \leq P(g_N)$ satisifty. Therefore P takes the maximal value at g_N, which is also the maximum value. And the maximum $P(g_N) = e^{-k_2 D} g(e^{-k_1 D}ET, g_N) + \frac{bET}{1+ET}$.

By proof (II), we can easily get that P takes the minimum value at $g = 0$, and the minimum value is $\frac{bET}{1+ET}$. This completes the proof. □

4. Periodic solution of system (2.2)

4.1. Boundary periodic solution

For system (2.2), if sterile mosquitoes are no longer released, the system has boundary periodic solution. At this point, we get the following system:

$$\begin{cases} \dfrac{dw(t)}{dt} = w(t)\left[\dfrac{rw(t)}{w(t)} - \varphi_1 - a_1(w(t))\right] = -a_1 w(t)^2 + (r - \varphi_1)w(t), \ w(t) < ET, \\ w(t^+) = Z_1(D)w(t), \ w(t) = ET. \end{cases} \tag{4.1}$$

The initial condition is $w(0^+) = e^{-k_1 D}ET$, and solving the above equation we get

$$w^T(t) = \frac{exp(tr)ET(r - \varphi_1)}{(r - \varphi_1)exp(t\varphi_1 + k_1 D) + a_1 ET[exp(tr) - exp(t\varphi_1)]}.$$

Suppose $w(t)$ reaches L_3 at time T, let $w(t) = ET$, we obtain:

$$ET = \frac{exp(rT)ET(r - \varphi_1)}{(r - \varphi_1)exp(T\varphi_1 + k_1 D) + a_1 ET[exp(rT) - exp(T\varphi_1)]}.$$

Further solve the above equation on T, where T represents the boundary periodic solution, we have

$$T = \frac{1}{r - \varphi_1} ln \frac{a_1 ET - e^{k_1 D}r + e^{k_1 D}\varphi_1}{a_1 ET - r + \varphi_1}, D = \frac{1}{k_1} ln \frac{a_1 ET - (a_1 ET - r + \varphi_1)e^{(r-\varphi_1)T}}{r - \varphi_1}.$$

Therefore, the boundary periodic solution of model (2.2) with period T is

$$\begin{cases} w^T(t) = \dfrac{exp[r(t - (k-1)T)]ET(r - \varphi_1)}{(r - \varphi_1)exp[\varphi_1(t - (k-1)T) + k_1 D] + a_1 ET}, \\ g^T(t) = 0. \end{cases} \tag{4.2}$$

Theorem 4.1. *If the condition $|\chi_1| < 1$ holds, then the boundary periodic solution of system* (2.2) *is orbitally asymptotically stable, where*

$$\chi_1 = \Delta_1 exp(I_1 - I_2). \tag{4.3}$$

where $\Delta_1 = \frac{e^{-k_2D}e^{-k_1D}(r-\varphi_1-a_1e^{-k_1D})}{r-\varphi_1-a_1ET}$, $I_1 = \frac{r-\varphi_1-\varphi_2}{r-\varphi_1} ln\frac{a_1ET-e^{k_1D}r+e^{k_1D}\varphi_1}{a_1ET-r+\varphi_1}$, $I_2 = (\frac{2a_1+a_2}{a_1})ln\left[1+\frac{r-\varphi_1-e^{k_1D}r+e^{k_1D}\varphi_1}{(a_1ET-r+\varphi_1)(r-\varphi_1)e^{-k_1D}}\right]$.

Proof. Let $F(w,g) = w(\frac{rw}{w+g} - \varphi_1 - a_1(w+g))$, $G(w,g) = -g(\varphi_2 + a_2(w+g))$, $\alpha(w,g) = w(e^{-k_1D} - 1)$, $\beta(w,g) = g(e^{-k_1D} - 1) + \frac{bET}{1+ET}$, $\Phi(w,g) = w - ET, (w^T(T), g^T(T)) = (ET, 0), (w^T(T^+), g^T(T^+)) = (e^{-k_1D}ET, 0)$.

Then

$$\frac{\partial F}{\partial w} = \frac{rwg}{(w+g)^2} + \frac{rw}{w+g} - 2a_1w - a_1g - \varphi_1, \frac{\partial G}{\partial g} = -\varphi_2 - a_2w - 2a_2g, \frac{\partial \alpha}{\partial w} = e^{-k_1D} - 1,$$
$$\frac{\partial \beta}{\partial g} = e^{-k_2D} - 1, \frac{\partial \Phi}{\partial w} = 1, \frac{\partial \alpha}{\partial g} = \frac{\partial \beta}{\partial w} = \frac{\partial \Phi}{\partial g} = 0.$$

$$\begin{aligned}
\Delta_1 &= \frac{F_+(\frac{\partial \beta}{\partial g}\frac{\partial \Phi}{\partial w} - \frac{\partial \beta}{\partial w}\frac{\partial \Phi}{\partial g} + \frac{\partial \Phi}{\partial w}) + G_+(\frac{\partial \alpha}{\partial w}\frac{\partial \Phi}{\partial g} - \frac{\partial \alpha}{\partial g}\frac{\partial \Phi}{\partial w} + \frac{\partial \Phi}{\partial g})}{F\frac{\partial \Phi}{\partial w} + G\frac{\partial \Phi}{\partial g}} \\
&= \frac{F_+(w^T(T^+), g^T(T^+))(1 + \frac{\partial \beta}{\partial g})}{F(w^T(T), g^T(T))} \\
&= \frac{e^{-k_2D}e^{-k_1D}(r - \varphi_1 - a_1e^{-k_1D}ET)}{r - \varphi_1 - a_1ET}
\end{aligned}$$

and

$$\begin{aligned}
exp\left(\int_0^T \left[\frac{\partial F}{\partial w}(w^T(T), g^T(T)) + \frac{\partial G}{\partial g}(w^T(T), g^T(T))\right] dt\right) &= exp\left(\int_0^T \left[r - \varphi_1 - \varphi_2 - (2a_1 + a_2)w^T(t)\right] dt\right) \\
&= exp(I_1 - I_2),
\end{aligned}$$

where

$$I_1 = (r - \varphi_1 - \varphi_2)T = \frac{r - \varphi_1 - \varphi_2}{r - \varphi_1} ln\frac{a_1ET - e^{k_1D}r + e^{k_1D}\varphi_1}{a_1ET - r + \varphi_1}$$
$$I_2 = (\frac{2a_1 + a_2}{a_1})ln\left[1 + \frac{r - \varphi_1 - e^{k_1D}r + e^{k_1D}\varphi_1}{(a_1ET - r + \varphi_1)(r - \varphi_1)e^{-k_1D}}\right].$$

Furthermore,

$$\begin{aligned}
\chi_1 &= \Delta_1 \exp\left(\int_0^T \left[\frac{\partial F}{\partial w}(w^T(T), g^T(T)) + \frac{\partial G}{\partial g}(w^T(T), g^T(T))\right] dt\right) \\
&= \Delta_1 exp(I_1 - I_2).
\end{aligned}$$

From article [45, Lemma 1], we know that if the condition $|\chi_1| < 1$ holds, the order-1 periodic solution of system (2.2) is orbitally asymptotically stable. This completes the proof. □

4.2. The existence and stability of periodic solution

From the Theorem 3.1, we get that system (2.2) must exist a fixed point of the Poincaré map, which represents system (2.2) exists an order-1 periodic solution. So we first talk about the stability of order-1 periodic solution $(\xi(t), \eta(t))$. Without loss of generality, we assume that the period of the order-1 periodic solution is T.

Theorem 4.2. *The order-1 period solution* $(\xi(t), \eta(t))$ *is orbitally asymptotically stable if*

$$\left|\frac{e^{-k_2D}e^{-k_1D}(\frac{re^{-k_1D}ET}{e^{-k_1D}ET+e^{-k_2D}\eta_0+\frac{bET}{1+ET}} - \varphi_1 - a_1(e^{-k_1D}ET + e^{-k_1D}\eta_0 + \frac{bET}{1+ET}))}{\frac{rET}{ET+\eta_0} - \varphi_1 - a_1(ET+\eta_0)} exp(\int_0^T Q(t)dt)\right| < 1, \qquad (4.4)$$

where $Q(t) = \frac{rwg}{(w+g)^2} + \frac{rw}{w+g} - 2a_1w - a_1g - \varphi_1 - \varphi_2 - a_2w - 2a_2g$.

Proof. We define the starting and the ending point of the order-1 periodic solutions as $(\xi(T), \eta(T)) = (ET, 0)$ and $(\xi(T^+), \eta(T^+)) = (e^{-k_1D}ET, e^{-k_2D}\eta_0 + \frac{bET}{1+ET})$ respectively.
Thus,

$$\begin{aligned}\Delta_1 &= \frac{F_+(e^{-k_1D}ET, e^{-k_2D}\eta_0 + \frac{bET}{1+ET})e^{-k_2D}}{F(ET,\eta_0)} \\ &= \frac{e^{-k_2D}e^{-k_1D}\left(\frac{re^{-k_1D}ET}{e^{-k_1D}ET+e^{-k_2D}\eta_0+\frac{bET}{1+ET}} - \varphi_1 - a_1(e^{-k_1D}ET + e^{-k_1D}\eta_0 + \frac{bET}{1+ET})\right)}{\frac{rET}{ET+\eta_0} - \varphi_1 - a_1(ET+\eta_0)},\end{aligned}$$

and

$$\int_0^T \left(\frac{\partial F}{\partial w} + \frac{\partial G}{\partial g}\right)dt = \int_0^T \left(\frac{rwg}{(w+g)^2} + \frac{rw}{w+g} - 2a_1w - a_1g - \varphi_1 - \varphi_2 - a_2w - 2a_2g\right)dt = \int_0^T Q(t)dt.$$

The multiplier χ_2 is obtained

$$\chi_2 = \Delta_1 exp\left(\int_0^T Q(t)dt\right).$$

From the (4.4), then $|\chi_2| < 1$ holds. By article [45, Lemma 1], we get that the order-1 periodic solution is orbitally asymptotically stable. This completes the proof. □

Theorem 4.3. *If* $P(g_N) < g_N$*, then system* (2.2) *has an globally asymptotically stable order-1 periodic solution.*

Proof. If $P(g_N) < g_N$, by Theorem 3.1 available Poincaré map P has a unique fixed point on $\overline{g}$, and $0 < \overline{g} \leq g_n$. This means that system (2.2) has a unique order-1 periodic solution that is orbitally asymptotically stable.

For any trajectory that starts at point $(e^{-k_1D}ET, g_0^+)$, if $g_0^+ \in [0, g_N]$, then $g_0^+ < P(g_0^+) < \overline{g}$ from the Theorem 3.1. After n times pulses, we get monotonically bounded sequence $P^n(g_0^+)$, then $\lim_{n\to+\infty} P^n(g_0^+) = \overline{g}$.

For any $g_0^+ > g_N$, we have two situations as follows: (a) for all n, if $P^n(g_0^+) > \overline{g}$, then with the increases of n, $P^n(g_0^+)$ monotonically decreases and $\lim_{n\to+\infty} P^n(g_0^+) = \overline{g}$ from the Theorem 3.1. (b) If

$P^n(g_0^+) > \overline{g}$ is not necessarily holds with all n, we make n_1 is the smallest positive integer and $P^{n_1}(g_0^+) < \overline{g}$. From the case (a), we get there must have a positive integer $n_2(n_2 > n_1)$, which makes $P^{n_2}(g_0^+)$ monotonically increases with the increase of n_2, therefore $\lim_{n_2 \to +\infty} P^{n_2}(g_0^+) = \overline{g}$. Thus, the unique order-1 periodic solution is globally asymptotically stable. This completes the proof.

□

Theorem 4.4. *When $P(g_N) > g_N, P^2(g_N) \geq g_N$, the system* (2.2) *has a stable order-1 periodic solution or a stable order-2 periodic solution.*

Proof. According to the Theorem 3.1, we get that P increases on $[0, g_N]$. So when $P(g_N) > g_N$, P has no fixed point on $[0, g_N]$. Then there is a positive integer j which satisfies $g_{j-1}^+ < g_N, g_j^+ \geq g_N$, by the definition of Poincaré map we obtain $g_j^+ = P(g_{j-1}^+) \leq P(g_N)$ and $g_j^+ \in [g_N, P(g_N)]$.

For $g_0^+ \in (g_N, +\infty)$, P is monotonically decreasing on $[g_N, +\infty)$, so $g_1^+ = P(g_0^+) \leq P(g_N)$. Then to any integer j such that $g_j^+ \in [g_N, P(g_N)]$. Therefore we get $g_j^+ \in [g_N, P(g_N)]$ always hold.

From P is monotonically decreasing on $[g_N, P(g_N)]$, P^2 is increasing on $[g_N, P(g_N)]$, thus

$$P([g_N, P(g_N)]) = [P^2(g_N), P(g_N)] \subset [g_N, P(g_N)].$$

Based on the above conclusions, for any $g_0^+ \in [g_N, P(g_N)]$, we assume that the $g_1^+ = P(g_0^+) \neq g_0^+, g_2^+ = P^2(g_0^+) \neq g_0^+, g_n^+ = P^n(g_0^+)$. This means the solution of model (2.2) starts from $(e^{-k_1 D}ET, g_0^+)$, which is not the order-1 and the order-2 periodic solution. In other words, if $g_1^+ = P(g_0^+) = g_0^+, g_2^+ = P^2(g_0^+) = g_0^+$, then P takes the fixed point at g_0^+, system (2.2) has both order-1 periodic solution and order-2 periodic solution. So we should discuss the parameters of $g_N, P(g_N), g_0^+, g_1^+ and\ g_2^+$. Thus, we discuss the following four cases:

(I) $P(g_N) \geq g_1^+ > g_0^+ > g_2^+ \geq g_N$. In this case (*Fig.3a*), $g_3^+ = P(g_2^+) > P(g_0^+) = g_1^+, g_2^+ = P(g_1^+) < P(g_3^+) = g_4^+$. So $g_3^+ > g_1^+ > g_0^+ > g_2^+ > g_4^+$. By summing up the above relations, we obtain

$$P(g_N) \geq ... > g_{2n+1}^+ > g_{2n-1}^+ > ... > g_1^+ > g_0^+$$

$$> g_2^+ > ... > g_{2n}^+ > g_{2n+2}^+ > ... \geq g_N.$$

(II) $P(g_N) \geq g_1^+ > g_2^+ > g_0^+ \geq g_N$. In this case (*Fig.3b*), we have $g_1^+ = P(g_0^+) > P(g_2^+) = g_3^+ > g_2^+ = P(g_1^+)$ and $P(g_2^+) = g_3^+ > g_4^+ = P(g_3^+) > P(g_1^+) = g_2^+$, therefore $g_1^+ > g_3^+ > g_4^+ > g_2^+ > g_0^+$. By induction, one obtains

$$P(g_N) \geq g_1^+ > ... > g_{2n-1}^+ > g_{2n+1}^+ > ...$$

$$> g_{2n+2}^+ > g_{2n}^+ > ... > g_2^+ > g_0^+ \geq g_N.$$

(III) $P(g_N) \geq g_0^+ > g_2^+ > g_1^+ \geq g_N$. Like case (2), we obtain

$$P(g_N) \geq g_0^+ > g_2^+ ... > g_{2n}^+ > g_{2n+2}^+ > ...$$

$$> g_{2n+1}^+ > g_{2n-1}^+ > ... > g_1^+ \geq g_N.$$

(IV)$P(g_N) \geq g_2^+ > g_0^+ > g_1^+ \geq g_N$. By using the similar process as case (1), we get

$$P(g_N) \geq ... > g_{2n+2}^+ > g_{2n}^+ > ... > g_2^+ > g_0^+$$

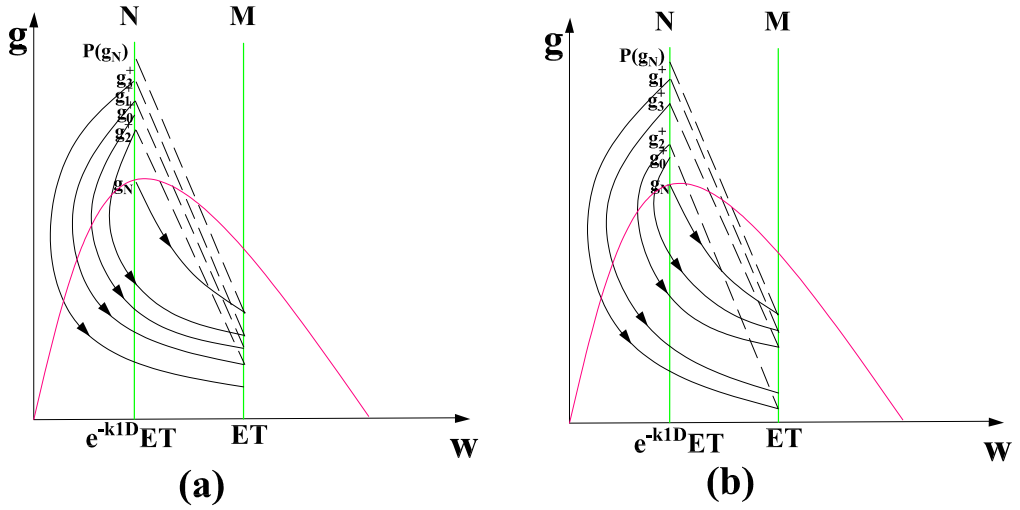

Figure 3. Path curve of system (2.2) (a)$P(g_N) \geq g_1^+ > g_0^+ > g_2^+ \geq g_N$ (b)$P(g_N) \geq g_1^+ > g_2^+ > g_0^+ \geq g_N$

$$> g_1^+ > ... > g_{2n-1}^+ > g_{2n+1}^+ > ... \geq g_N.$$

For case (II) and (III), we know that $P^{2n}(g_0^+) = g_{2n}$ is monotonically increasing and $P^{2n+1}(g_0^+) = g_{2n+1}^+$ is monotonically decreasing. So there exists a unique $\overline{g}$ that makes

$$\lim_{n\to+\infty} g_{2n+1}^+ = \lim_{n\to+\infty} g_{2n}^+ = \overline{g}, \quad \overline{g} \in [g_N, P(g_N)].$$

Or there exists two fixed values $\overline{g}_1, \overline{g}_2 \in [g_N, P(g_N)]$ and $\overline{g}_1 \neq \overline{g}_2$ such that

$$\lim_{n\to+\infty} g_{2n+1}^+ = \overline{g}_1, \lim_{n\to+\infty} g_{2n}^+ = \overline{g}_2.$$

For case (I) and (IV), only the second case is satisfied.

Thus, system (2.2) has an order-1 or order-2 periodic solution for case (II) and case (III), has an order-2 periodic solution for case (I) and case (IV). This completes the proof. □

Theorem 4.5. *When $P(g_N) > g_N, P^2(g_N) < g_{min}^+$, where $g_{min}^+ = min\{g^+, P(g^+) = g_N\}$. Then model* (2.2) *has a nontrivial order-3 periodic solution. And system* (2.2) *exist order-k ($k \geq 3$) periodic solution.*

Proof. When $P(g_N) > g_N$, the Poincaré map have a unique fixed point $\overline{g}$ and $\overline{g} \in (g_N, P(g_N))$. In order to study the existence of order-3 periodic solution, we need to get a fixed point $\widetilde{g} \in [0, +\infty)$ such that $P^3(\widetilde{g}) = \widetilde{g}$ and $P(\widetilde{g}) \neq \widetilde{g}$. By the Theorem 3.1 $P^3(g)$ is continuous on $[0, +\infty)$, therefore $P^3(0) = P^2(\frac{bET}{1+ET}) > 0$ and $P^3(g_{min}^+) = P^2(g_N) < g_{min}^+$.

Further, it follows from the intermediate value theorem and the continuity of P^3, system (2.2) must have a positive point $\widetilde{g} \in (0, g_{min}^+)$ where $P^3(\widetilde{g}) = \widetilde{g}$ and $g_{min}^+ < g_N$. We can easily get that $\widetilde{g} \neq g_N$.

Therefore, system (2.2) has an order-3 periodic solution. From Sarkovskii [46] theorem and [45, Definition 2] that the order-k periodic solution exists on system (2.2). This complete the proof. □

5. Numerical simulations

In the section 4, we obtain the boundary periodic solution of system (2.2) and the expressions of T and D. Therefore, we can analyze the key factors T and ET that affect the dose D of insecticides. Let $r = 2.5, \varphi_1 = 0.2, a_1 = 0.3, \varphi_2 = 0.01, a_2 = 0.05$, we get when the threshold ET increases, the insecticides dose D decreases, and the downward trend becomes more and more obvious ($Fig.4a$). Further, when the period T increases, the insecticides dose D also increases ($Fig.4b$). Therefore, the effects of ET and T should be taken into account in the actual dose of insecticide sprayed.

We use the boundary periodic solution stability condition (4.3) to determine whether the wild mosquito population can be controlled by chemical control alone, that is, $\chi_1 < 1$ means that the wild mosquito population can be controlled below ET under the conditions of only chemical control. Therefore, we use numerical simulation to study the effect of threshold ET on stability condition $\chi_1(Fig.5)$, where the parameter values are $r = 2.5, \varphi_1 = 0.2, a_1 = 0.3, \varphi_2 = 0.01, a_2 = 0.05, k_1 = 1.6, D = 1.6$. From the Fig.5, we get $\chi_1 < 1$ when ET is relatively small, and $\chi_1 > 1$ when ET increases to a certain value. This indicates that when the value of a is fixed, a smaller ET value is more conducive to controlling the wild mosquito population. And the early use of chemical control makes the control of wild mosquitoes. But when the ET get large, repeated chemical controls can make wild mosquito populations resistant and cannot be effectively controlled. So the use of integrated mosquito control is a reasonable and effective method.

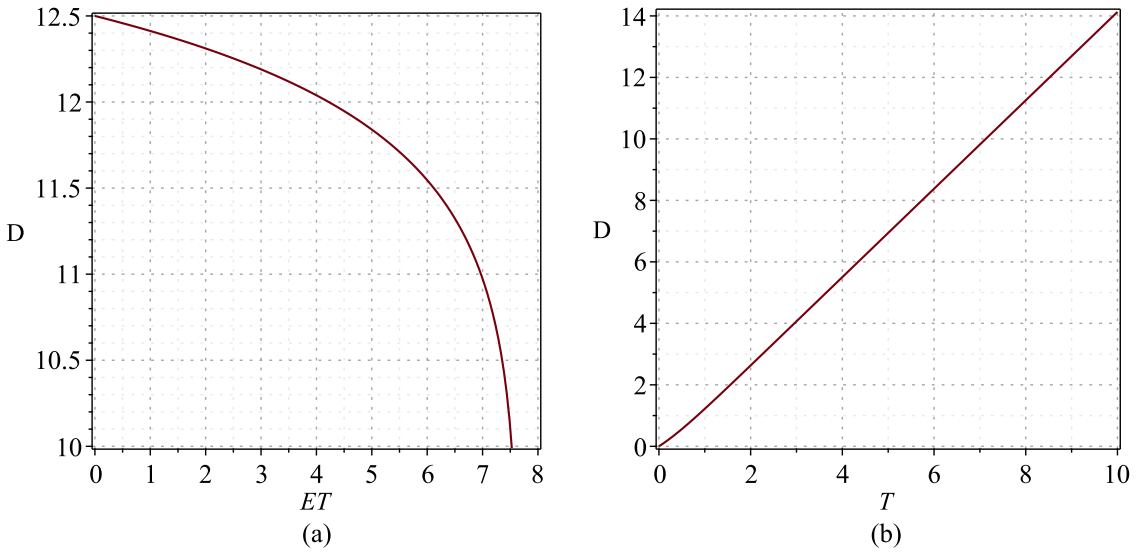

Figure 4. The influence of key factors ET, T on insecticide dose D: (a)$r = 2.5, \varphi_1 = 0.2, a_1 = 0.3, \varphi_2 = 0.01, a_2 = 0.05, k_1 = 1.6, T = 8.6956$;(b)$r = 2.5, \varphi_1 = 0.2, a_1 = 0.3, \varphi_2 = 0.01, a_2 = 0.05, k_1 = 1.6, ET = 2.5$.

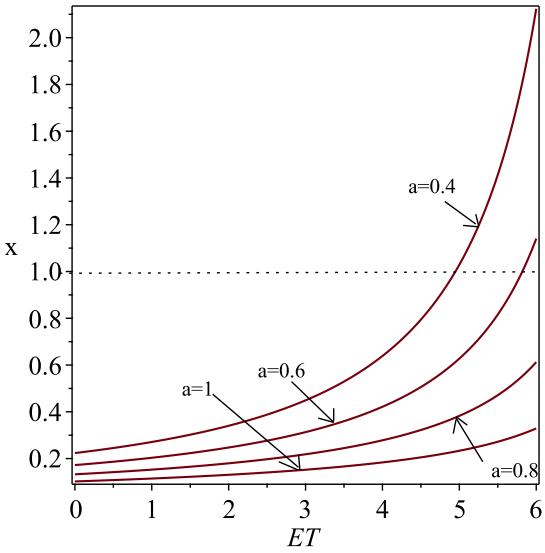

Figure 5. The influence of key factors ET on the stability condition χ_1 :$r = 2.5, \varphi_1 = 0.2, a_1 = 0.3, \varphi_2 = 0.01, a_2 = 0.05, k_1 = 1.6, D = 1.6$.

Let parameters $r = 2.5, \varphi_1 = 0.2, a_1 = 0.3, \varphi_2 = 0.01, a_2 = 0.05, ET = 2.5$, we get that system (2.2) has order-1 periodic solution and it is globally asymptotically stable ($Fig.6a$). Figure (6b) and (6c) are time series diagram of w, g. The results show that the wild mosquito population can be controlled below the threshold ET when using integrated mosquito control.

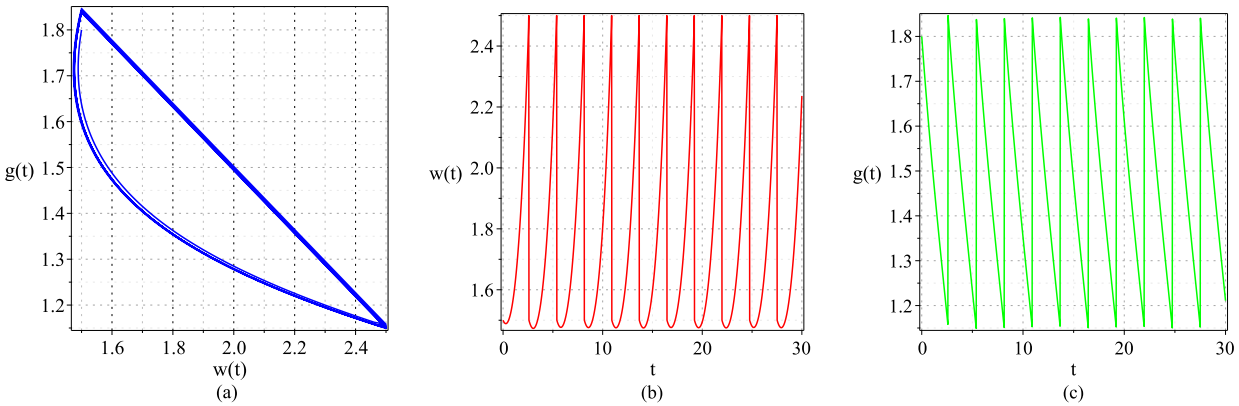

Figure 6. Periodic solution and time series of system (2.2) under state pulses. We let $r = 2.5, \varphi_1 = 0.2, a_1 = 0.3, \varphi_2 = 0.01, a_2 = 0.05$.

6. Conclusion

In this paper, we present the wild and sterile mosquito system with state-dependent feedback control and study its global dynamics. According to the introduction and main results of the article, system (2.2) using state-dependent feedback control is not only practical, but also rich in dynamic behavior.

In the article we define the Poincaré map P and study its main properties such as monotonicity,

continuity, extremum, and fixed point. We obtain an expression for the boundary period solution with the period T and the pesticide dose D, which proves that it is stable under certain conditions. Based on the properties of Poincaré map, we prove the existence and stability of the order-1 periodic solution of system(2.2), and solve the dynamic complexity of the system, such as the proof of the existence of the order-3 periodic solution.

We use numerical simulations to verify the impact of key parameters and validate our conclusions. By analyzing the key influencing factors of pesticide D, we get that when the threshold ET increases, D decreases continuously, and when the period T increases, D increases continuously. Therefore, the dose of pesticide should consider the effects of ET and T at the same time. By studying the influence of threshold ET on the stability condition χ_1 of the boundary period, we get that the population of wild mosquitoes cannot be effectively controlled when ET is large. This verifies the necessity of adopting an integrated mosquito control. Through numerical simulation, we verify the existence and stability of the order-1 periodic solution. That is, through integrated mosquito control, wild mosquitoes can be controlled below the threshold.

Compared with the previous state-dependent feedback control model, we summarize some of the highlights of this paper: (1) We study the global dynamics of the model through the properties of the Poincaré map, and the existence of periodic solution is proved by studying the fixed point of Poincaré map. (2) The biological control method used in this paper is sterile insect technique. And wild mosquito populations can be more effectively controlled by using a new proportional release method when releasing sterile mosquitoes. (3) We study the effects of insecticide dose on integrated mosquito control and the influence of key parameters is analyzed by numerical simulation. In future research work, we will add optimization problems to reduce control costs.

Acknowledgments

This work is supported by the National Natural Science Foundation of China (11371230), the SDUST Research Fund (2014TDJH102), Shandong Provincial Natural Science Foundation, China (ZR2015AQ001), Joint Innovative Center for Safe And Effective Mining Technology and Equipment of Coal Resources, SDUST Innovation Fund for Graduate Students (SDKDYC170225), SDUST Innovation Fund for Graduate Students(SDKDYC190351).

Conflict of interest

The authors declare that there is no conflict of interests regarding the publication of this paper.

References

1. K. Ciesielski, On stability in impulsive dynamical systems, *B. Pol. Acad. Sci. Math.*, **52** (2010), 81–91.
2. Z. Shi, Y. Li and H. Cheng, Dynamic analysis of a pest management smith model with impulsive state feedback control and continuous delay, *Mathematics* , **7** (2019), 591.
3. T. Zhang, X. Liu, X. Meng, et al., Spatio-temporal dynamics near the steady state of a planktonic system, *Comput. Math. Appl.*, **75** (2018), 4490–4504.

4. Y. Li, H. Cheng, J. Wang, et al., Dynamic analysis of unilateral diffusion Gompertz model with impulsive control strategy, *Adv. Differ. Equ.*, **2018** (2018), 32.
5. J. Wang, H. Cheng, H. Liu, et al., Periodic solution and control optimization of a prey-predator model with two types of harvesting, *Adv. Differ. Equ.*, **2018** (2018), 1687–1847.
6. N. Gao, Y. Song, X. Wang, et al., Dynamics of a stochastic SIS epidemic model with nonlinear incidence rates, *Adv. Differ. Equ.*, **2019** (2019), 41.
7. Y. Li, H. Cheng and Y. Wang, A Lycaon pictus impulsive state feedback control model with Allee effect and continuous time delay, *Adv. Differ. Equ.*, **2018** (2018), 1687–1847.
8. L. Zhang, Y. Wang, M. Khalique, et al., Peakon and cuspon solutions of a generalized Camassa-Holm-Novikov equation, *J. Appl. Anal. Comput.*, **8** (2018).
9. Z. Shi, J. Wang, Q. Li, et al., Control optimization and homoclinic bifurcation of a preyCpredator model with ratio-dependent, *Adv. Differ. Equ.*, **7** (2019), 591.
10. K. Liu, T. Zhang and L. Chen, State-dependent pulse caccination and therapeutic strategy SI epidemic model with nonlinear incidence rate, *Comput. Math. Method. M.*, **2019** (2019), 10.
11. W. Lv and F. Wang, Adaptive tracking control for a class of uncertain nonlinear systems with infinite number of actuator failures using neural networks, *Adv. Differ. Equ.*, **2017** (2017), 374.
12. H. Liu and H. Cheng, Dynamic analysis of a prey-predator model with state-dependent control strategy and square root response function, *Adv. Differ. Equ.*, **2018** (2018), 63.
13. F. Wang, B. Chen, Y. Sun, et al., Finite time control of switched stochastic nonlinear systems, *Fuzzy Set. Syst.*, **365** (2019), 140–152.
14. X. Meng, F. Li and S. Gao, Global analysis and numerical simulations of a novel stochastic eco-epidemiological model with time delay, *Appl. Math. Comput.*, **339** (2018), 701–726.
15. Y. Ren, M. Tao, H. Dong, et al., Analytical research of (3 + 1)-dimensional Rossby waves with dissipation effect in cylindrical coordinate based on Lie symmetry approach, *Adv. Differ. Equ.*, **9** (2019), 13.
16. J. Wang, H. Cheng, X. Meng, et al., Geometrical analysis and control optimization of a predator-prey model with multi state-dependent impulse, *Adv. Differ. Equ.*, **2017** (2017), 252.
17. Y. Li, Y. Li, Y. Liu, et al., Stability analysis and control optimization of a prey-predator model with linear feedback control, *Discrete Dyn. Nat. Soc.*, **2018** (2018), 12.
18. G. Liu, X. Wang and X. Meng, Extinction and persistence in mean of a novel delay impulsive stochastic infected predator-prey system with jumps, *Complexity*, **2017** (2017), 115.
19. F. Wang and X. Zhang, Adaptive finite time control of nonlinear systems under time-varying actuator failures, *IEEE T. Syst.*, (2019).
20. J. Li, L. Cai and Y. Li, Stage-structured wild and sterile mosquito population models and their dynamics, *J. Biol. Dynam.*, **11** (2016), 1.
21. W. Mylene, L. Georges, M. Knud, et al., Comparative genomics: Insecticide resistance in mosquito vectors, *Nature*, **423** (2003), 136–7.
22. L. Zhang and M. Khalique, Classification and bifurcation of a class of second-order ODEs and its application to nonlinear PDEs, *Discrete Cont. Dyn. S*, **11** (2017), 777–790.

23. F, Liu, Continuity and approximate differentiability of multisublinear fractional maximal functions, *Math. Inequal. Appl.*, **21** (2018), 25–40.
24. P. Stiling, Biological control by natural enemies, *Ecology*, **73** (1992), 1520–1520.
25. A. C. Redfield, The biological control of chemical factors in the environment, *Sci Prog*, **11** (1960), 150–170.
26. Y. Li and X. Liu, H-index for nonlinear stochastic systems with state and input dependent noises, *Int. J. Fuzzy Syst.*, **20** (2018), 759–768.
27. F. Zhu, X. Meng and T. Zhang, Optimal harvesting of a competitive n-species stochastic model with delayed diffusions, *Math. Biosci. Eng.*, **16** (2019), 1554–1574.
28. L. Marshall, J. W. Miles and A. Press, Integrated mosquito control methodologies, (1983).
29. H. J. Barclay, Models for the sterile insect release method with the concurrent release of pesticides, *Ecol. Model.*, **11** (1980), 167–177.
30. Y. Li and X. Meng, Dynamics of an impulsive stochastic nonautonomous chemostat model with two different growth rates in a polluted environment, *Discrete Dyn. Nat. Soc.*, **2019** (2019), 15.
31. Y. Liu, H. Dong and Y. Zhang, Solutions of a discrete integrable hierarchy by straightening out of its continuous and discrete constrained flows, *Anal. Math. Phys.*, **2** (2018), 1–17.
32. W. Klassen, C. F. Curtis, W. Klassen, et al., Sterile Insect Technique, (1989).
33. M. Q. Benedict and A. S. Robinson, The first releases of transgenic mosquitoes: an argument for the sterile insect technique, *Trends Parasitol.*, **19** (2003), 349–355.
34. F. Liu, Q. Xue and K. Yabuta, Rough maximal singular integral and maximal operators supported by subvarieties on Triebel-Lizorkin spaces, *Nonlinear Anal.*, **171** (2018), 41–72.
35. T. Feng, Z. Qiu, X Meng, et al., Analysis of a stochastic HIV-1 infection model with degenerate diffusion, *Appl. Math. Comput.*, **348** (2019), 437–455.
36. L. Alphey, M. Benedict, R. Bellini, et al., Sterile-insect methods for control of mosquito-borne diseases: an analysis, *Vector Borne Zoonot. Dis*, **10** (2010), 295–311.
37. Y. Li, W. Zhang and X.Liu, H-index for discrete-time stochastic systems with Markovian jump and multiplicative noise, *Automatica*, **90** (2018), 286–293.
38. L. Zhang, Y. Wang, M. Khalique, et al., Peakon and cuspon solutions of a generalized Camassa-Holm-Novikov equation, *J. Appl. Anal. Comput.*, **8** (2018), 1938–1958.
39. J. Li and Z. Yuan, Modelling releases of sterile mosquitoes with different strategies, *J. Biol. Dyn.*, **9** (2015), 1–14.
40. H. Barclay and M. Mackauer, The sterile insect release method for pest control: a density-dependent model, *Environ. Entomol.*, **9** (1980), 810–817.
41. F. Wang, B. Chen, Y. Sun, et al., Finite time control of switched stochastic nonlinear systems, *Fuzzy Set. Syst.*, (2018).
42. H. Qi, X. Leng, X. Meng, et al., Periodic Solution and Ergodic Stationary Distribution of SEIS Dynamical Systems with Active and Latent Patients, *Qual. Theory Dyn. Syst.*, **18** (2019).
43. M. Huang, X. Song and J. Li, Modelling and analysis of impulsive releases of sterile mosquitoes, *J. Biol. Dynam.*, **11** (2017), 1147.

44. J. C. Panetta, A mathematical model of periodically pulsed chemotherapy: Tumor recurrence and metastasis in a competitive environment, *B. Math. Biol.*, **58** (1996), 425–447.

45. S. Tang, B. Tang, A. Wang, et al., Holling II predator–prey impulsive semi-dynamic model with complex Poincaré map, *Nonlinear Dynam.*, **81** (2015), 1575–1596.

46. D. R. J. Chillingworth, An Introduction to Chaotic Dynamical Systems by Robert L. Devaney, 1986.

AIMS Press